

Article

Alginate-Based Zinc Oxide Nanoparticles Coating Extends Storage Life and Maintains Quality Parameters of Mango Fruits “cv. Kiett”

Ibrahim Hmam^{1,*} , Mohamed Abdel-Shakur Ali²  and Abdou Abdellatif¹ ¹ Pomology Department, Faculty of Agriculture, Cairo University, Giza 12613, Egypt² Biochemistry Department, Faculty of Agriculture, Cairo University, Giza 12613, Egypt

* Correspondence: ibrahim.s.hmmam@agr.cu.edu.eg

Abstract: In this study, we describe the synthesis of zinc oxide nanoparticles (ZnO NPs) and evaluate the impact of alginate-based ZnO NPs (Alg–ZnO NPs) on microbiological activity, storage behavior, and physico-chemical properties of ‘Kiett’ mango fruit. The fruits were coated with alginate and Alg–ZnO NPs and then stored at 13 °C; uncoated mango fruits were used as controls. ZnO NPs were synthesized and characterized, confirming the formation of spherically shaped particles with sizes ranging from 12 to 15.1 nm and a zeta potential equal to 31 mV. Alg–ZnO NPs exhibited the same inhibition capacities against the growth of *E. coli* and *S. aureus* bacteria. The cold-stored fruits showed an increase in weight loss, respiration rate, total soluble solids (TSS), total sugars, and total carotenoids over the storage period. However, this increase was comparatively less significant in coated fruits than in uncoated ones. Alg–ZnO NP treatment maintained better fruit quality, controlled the decay incidence, and increased the shelf life of the mango fruits. Firmness and titratable acidity (TA) significantly decreased during storage, but this decrease was reduced in coated fruits. We conclude that Alg–ZnO NP treatment could be a promising safe alternative for maintaining fruit quality, extending the storage period, and increasing the shelf life of mango fruits ‘cv. Kiett’.

Keywords: *Mangifera indica*; edible coating; alginate; ZnO NPs; nanoparticle characterization; cold storage



Citation: Hmam, I.; Ali, M.A.-S.; Abdellatif, A. Alginate-Based Zinc Oxide Nanoparticles Coating Extends Storage Life and Maintains Quality Parameters of Mango Fruits “cv. Kiett”. *Coatings* **2023**, *13*, 362. <https://doi.org/10.3390/coatings13020362>

Academic Editor: Daniele Carullo

Received: 8 January 2023

Revised: 25 January 2023

Accepted: 29 January 2023

Published: 5 February 2023



Copyright: © 2023 by the authors. Licensee MDPI, Basel, Switzerland. This article is an open access article distributed under the terms and conditions of the Creative Commons Attribution (CC BY) license (<https://creativecommons.org/licenses/by/4.0/>).

1. Introduction

Mangoes (*Mangifera indica* L. Family: Anacardiaceae) are one of the most popular and economically important fruit crops in the tropical and subtropical regions for production and international trade [1]. Mango fruits are characterized by their attractive appearance, delicious taste and flavor, and high nutritional value [2]. Mango pulp is rich in several bioactive compounds, i.e., fiber, amino acids, carbohydrates, minerals, organic acids, vitamins, carotenoids, and polyphenolics [3] whose amount is highly influenced by cultivar, maturity stage, postharvest handling, and storage [4]. The worldwide production of mangoes is 54.73 million tons; India ranks as the top mango producer, contributing to 45.22% of the total mango production, followed by Indonesia (6.61%), Mexico (4.34%), China (4.33%), and Pakistan (4.28%).

Mango is a popular fruit crop in Egypt and is grown in several places. The most popular Egyptian mango cultivars are Alphonso, Ewais Mabroka, Hindi Besennara, Succary, and Zebda [5]. Kiett is a mango cultivar introduced to Egypt from Florida; Kiett is a late-season cultivar with large fruits (600–800 g). The Kiett cultivar has a green peel color and orange-yellow pulp with high TSS and no fibers at the fully mature stage [6]. Mango production and international trade are expanding rapidly; however, poor handling, high susceptibility to chilling injury, postharvest disease infection, and short storage life seriously reduce mangoes’ commercial value and limit international marketing [1,7]. Mangoes are a tropical fruit that is traditionally harvested when it is hard and green and ripens quickly

at room temperature [8]. As a respiratory climacteric fruit, mangoes undergo various biochemical changes that are initiated by the autocatalytic production of ethylene; these changes include increased respiration, weight loss, softening, and changes in carbohydrates, organic acids, and volatile compounds [3,8–10].

Because mango fruits are highly perishable, significant postharvest losses may occur during the harvesting, transporting, and marketing stages [11]. Many scholars have found that mango fruit losses after harvest can be as high as 50% in developing countries where handling and storage methods are not ideal [3,12]. Harvesting at an improper maturity stage, poor fruit handling, mechanical damage, improper packaging, inadequate storage facilities, and sensitivity to chilling injuries, disease, and pest damage are significant causes of postharvest losses [13,14]. Hence, the appropriate postharvest technologies play a pivotal role in reducing mango fruit losses, maintaining mango fruit quality, and extending mango postharvest shelf life [3].

Coatings are one of the promising techniques for extending the storage shelf life of mango fruits; they can enhance the appearance, improve fruit quality, delay ripening, and prolong shelf life [7,15]. The application of edible coatings offers an attractive, safe, and eco-friendly approach to fruit preservation [16–18]. The edible coating acts as a barrier to gas diffusion, depresses respiration rate, retards water loss, maintains sensory attributes, retards fruit ripening, and extends storage life [19,20]. Edible coatings of natural origin are considered a safe, non-toxic approach for fruit preservation [19]. Sodium alginate (SA), a natural polysaccharide obtained from brown seaweeds [21], has been widely used as an edible coating; SA is generally recognized as a safe polysaccharide with excellent film-forming properties, selective gas permeabilities, low cost, biodegradability, and non-toxicity characteristics [22,23].

The application of nanoparticles is a new technique for extending the shelf life of fresh fruits [24]. Nanoparticles have unique physical and chemical characteristics in addition to their antioxidant and antimicrobial activity [25–27]. Among the metal oxides, ZnO NPs are considered the most promising nanoparticles due to their unique physicochemical properties, biocompatibility, low production costs, and excellent bioactivity [28,29]. ZnO NPs have been recognized as a safe coating material by the Food and Drug Administration of the United States with no potential threat to human health [29,30].

Recently, coating materials loaded with nanoparticles emerged as a promising and safe postharvest technique that maintains quality properties with less penetration of nanoparticles into the treated product [31,32]. Therefore, the present investigation aimed to evaluate the applicability of alginate-based ZnO NPs as a coating on microbial activity, storage behavior, and physicochemical properties of mango fruits.

2. Materials and Methods

2.1. Preparation of Zinc Oxide Nanoparticles

Zinc oxide nanoparticles (ZnO NPs) were synthesized using a solvothermal synthesis process [33,34]. Briefly, a zinc acetate solution was prepared by dissolving 1.48 g of zinc acetate (LOBA Chemie PVT. LTD., Mumbai, India) in 63 mL of absolute ethanol (Chem-Lab., Zedelgem, Belgium) with constant stirring at 60 °C; 0.74 g of KOH (Merck Darmstadt, Germany) was dissolved in 33 mL of absolute ethanol under the same conditions. KOH was added dropwise into the zinc acetate solution with vigorous stirring and heating to 60 °C. The mixture was heated to 60 °C and stirred for three hours until the reaction was complete. A white precipitate (ZnO NPs) was formed and collected by centrifugation at 4000 rpm for 10 min, then washed with acetone and ultrapure water to remove all the impurities. The ZnO NPs were dried overnight in an oven at 60 °C.

2.2. Characterization of ZnO NPs

2.2.1. Particle Size and Zeta Potential

The particle size and zeta potential of the nanoparticles were measured by photon correlation spectroscopy and laser Doppler anemometry, respectively, using a Zetasizer[®] 3000

(Malvern Instruments, Malvern, UK) in the central lab of the Faculty of Pharmacy, Cairo University, Egypt. Briefly, the size measurement was performed three times at 25 °C/90° scattering angle, and each measurement was recorded for 3 min. The mean hydrodynamic diameter was generated by cumulative analysis. The zeta potential measurements were performed using an aqueous dip cell in the automatic mode.

2.2.2. Transmission Electron Microscopy (TEM)

The morphological examination of the synthesized nanoparticles was performed by transmission electron microscopy (JEOL JEM-1400, Peabody, MA, USA). A drop (2 µL) of water containing dissolved synthesized nanoparticles was placed on a carbon grid. The images were obtained at a bias voltage of 40–120 kV and used to analyze samples at the Cairo University Research Park (CURP), Egypt. The size was obtained by measuring the diameter of particles in the TEM images.

2.2.3. Scanning Electron Microscopy (SEM) and Energy-Dispersive X-ray Spectroscopy (EDX)

Zinc oxide nanoparticles (ZnO NPs) were coated with gold using a S150A Sputter Coater (Edwards, England); then, the morphology and topography of the prepared nanoparticles were analyzed by field emission scanning electron microscopy (FE-SEM; Quanta FEG 250, Netherland, Holland) at the Electron Microscopy Unit of the National Research Centre, Egypt. The elemental composition of the sample was determined by energy-dispersive X-ray spectroscopy using the software (TEAM) built into the scanning electron microscope.

2.2.4. Fourier Transform Infrared Spectroscopy

The association level between the materials during ZnO NPs synthesis was evaluated. The ZnO NPs powder was prepared by milling to form a very fine powder that was then placed on the device grid for measurement. The infrared spectra were recorded with a Fourier-transform infrared (FTIR) spectroscopy analyzer (VERTEX 80v, BRUKER, Ettlingen, Germany) at the Central Lab of the National Research Centre, Egypt within the scanning range of 4000–400 cm⁻¹. The spectra were smoothed using 3 or 5 points and the baseline of the spectra was corrected using the previously recorded spectra of the sample. As a reference, the background spectrum of air was collected before the acquisition of the sample spectrum.

2.3. Antimicrobial Properties of Alg–ZnO NPs

The antimicrobial activity of the Alg–ZnO NPs was evaluated against Gram-positive *Escherichia coli* (O157:H7 wild type strain 93,111), obtained from the Cairo University Research Park (CURP), Egypt, and Gram-negative *Staphylococcus aureus* (ATCC25923) bacteria using the well diffusion method [35]. One mL of bacterial culture was transferred into a sterilized petri dish filled with Mueller Hinton agar medium. After the culture medium was completely solidified, three wells with a 10 mm diameter were punched. A total of 100 µL of 1% Alg–ZnO NP solution (*w/v*) was dispensed into the small wells, and the plates were incubated at 37 °C for 24–48 h; polymyxin at the same volume and concentration was used in the control group. The antibacterial properties of the samples were quantitated by measuring the diameter of inhibition zone in millimeters (mm).

2.4. Preparation of Alginate Coatings

For the preparation of a 1.5% sodium alginate (SA) solution, SA powder (15 g/L) (LOBA Chemie PVT. LTD., Mumbai, India) was stirred at 50 °C until the sodium alginate powder was completely dissolved [36]. Glycerol (3 g/L) (LOBA Chemie PVT. LTD., Mumbai, India) was added to the solutions as a plasticizer [37]. Calcium chloride was prepared to induce the cross-linking reaction; CaCl₂ (30 g/L) (Merck Darmstadt, Germany) was dissolved in distilled water at room temperature until the mixture became clear. To prepare the 0.5% alginate-based ZnO NPs (Alg–ZnO NPs), 5 g of white ZnO NP powder

was slowly added into the above-prepared alginate solution under magnetic stirring at ambient temperature to form a uniform suspension.

2.5. Fruits Material

Freshly harvested mango (cv. Kiett) fruits were obtained from a commercial mango orchard located in Ismailia governorate, Egypt, with well-managed conditions. Mango fruits that were mature, homogeneously sized (~750 g), and free of mechanical injury were picked early in the morning and transported to the postharvest laboratory of the Pomology Department, Faculty of Agriculture, Cairo University. The fruits were carefully washed in tap water and kept at ambient temperature to dry.

2.6. Coating Application and Storage Conditions

For coating treatment, mango fruits were divided into three groups, each containing 60 fruits. The fruits were completely immersed for one minute in the coating solutions. Fruits in the first group were immersed in 1.5% SA and fruits in the second group were immersed in Alg-ZnO NPs, and the excess coating solution allowed to drip off. After that, the fruits were dipped in a 3% calcium chloride solution for 3 min and left to dry for one hour at room temperature (25 °C). Fruits in the third group were left without coating as a control. All mango fruits were packed in carton boxes, eight fruits/box, and stored in a cold chamber at 13 °C with 85%–90% RH for 28 days, followed by 7 days of shelf life at 22 °C and 85%–90% RH.

The fruit quality assessment of each treatment was evaluated regularly after 0, 7, 14, 21, and 28 days. Then, the fruit quality assessment was also conducted after the additional 7 days at 22 °C (shelf life).

2.7. Fruit Quality Assessment

2.7.1. Respiration Rate

Three mango fruits from each treatment were placed separately in an airtight jar (18 cm diameter × 25 cm height) for 24 h at 13 °C (cold storage conditions) or 22 °C (shelf life conditions) to measure the respiration rate. A gas sample was measured for oxygen and carbon dioxide analysis using a YesAir (8-channel IAQ monitor, Critical-Environment Technologies, Delta, BC, Canada) supplemented with O₂ and CO₂ gas sensors. The respiration rate was calculated according to Pristijono et al. [38] and expressed as nmol CO₂ kg⁻¹ s⁻¹.

2.7.2. Weight Loss

The initial mango fruit weight ($n = 10$) of each treatment was determined at the beginning of storage (W_i) and was periodically weighted at each sampling date (W_s); weight loss (%) was calculated according to Shah and Hashmi [20] by the following equation (Equation (1)):

$$\text{Weight loss (\%)} = (W_i - W_s) / W_i \times 100 \quad (1)$$

2.7.3. Fruit Pulp Firmness

Fruit pulp firmness ($n = 6$) of fruits from each treatment was measured using a fruit hardness tester (Lutron FR-5120, Electronic Enterprise, Taipei, Taiwan) equipped with a 5 mm-diameter cylindrical probe. The entire fruit was placed on a flat surface, and firmness was measured on the palled fruit surface in the equatorial zone. The results were expressed in Newtons (N) [39].

2.7.4. Total Soluble Solids (TSS), Titratable Acidity (TA) and TSS/TA Ratio

Mango fruit juice for each treatment was used to determine TSS and TA according to the method of Islam et al. [40]. TSS concentration was measured using a digital refractometer (Atago, Model PAL-1, Tokyo, Japan), and the data were expressed as °Brix. The TA (%) of the fruit pulp was measured by titrating 10 mL of aliquoted juice (1 mL

juice + 9 mL distilled water) with 0.1 mol NaOH (Merck Darmstadt, Darmstadt, Germany) using a phenolphthalein indicator until a permanent pink color appeared; total acidity was expressed as a percentage of citric acid equivalent based on fresh weight. By dividing the TSS percent with the corresponding acidity percentage, the TSS/TA ratio was calculated.

2.7.5. Total Sugars Content

Total sugar content was determined by the phenol–sulfuric acid method [41]. Fruit pulp samples (0.25 g) were homogenized in 20 mL 70% ethanol (Chem-Lab., Zedelgem, Belgium); 1 mL of the ethanolic extract was treated with 1 mL of 5% phenol (*w/v*) (LOBA Chemie PVT. Ltd., Mumbai, India) and 5 mL of 98% sulfuric acid (Adwic Pharmaceutical Co., Cairo, Egypt). The absorbance of the developed color was measured at a wavelength of 490 nm using a spectrophotometer (JENWAY, Model 6300, Staffordshire, UK). A standard curve was generated using a pure glucose solution, and total sugar content was expressed as mg glucose equivalent per g of pulp fresh weight.

2.7.6. Reducing Sugar Content

Reducing sugar content was determined by the dinitrosalicylic acid (DNS) method [42]. The dinitrosalicylic acid (DNS) reagent was prepared by dissolving 1.0 g of DNS (LOBA Chemie PVT. Ltd., Mumbai, India), 200 mg of crystalline phenol (LOBA Chemie PVT. Ltd., Mumbai, India), and 50 mg of sodium sulphate (LOBA Chemie PVT. Ltd., Mumbai, India) in 100 mL of 1% NaOH (Merck Darmstadt, Germany) by stirring at room temperature. One mL of the alcohol extract, 3 mL distilled water, 3 mL of DNS reagent were mixed and heated in a boiling water bath for 5 min. A total of 1 mL of 40% Rochelle salt (sodium–potassium tartrate salt) (ADVENT CHEMBIO PVT LTD, Mumbai, India) solution was added after the color had developed. The final absorbance of the set color was measured at 575 nm using a spectrophotometer (JENWAY, Model 6300, Staffordshire, UK). The reducing sugar content results were expressed as mg glucose equivalent per g of fresh weight.

2.7.7. Total Carotenoid Content

Fruit pulp samples (0.5 g) were homogenized in 20 mL of 80% acetone (LOBA Chemie PVT. Ltd., Mumbai, India) in a dark glass bottle at room temperature. The absorbance was measured using a UV–visible spectrophotometer (JENWAY, Model 6300, Staffordshire, UK) at the wavelengths of 480 and 510 nm. Total carotenoid content was calculated according to Himmam [32] as $\mu\text{g g}^{-1}$ of fresh weight.

2.7.8. Total Phenol Content

Total phenol concentration was determined spectrophotometrically using the Folin–Ciocalteu colorimetric method [43] with a slight modification. To do this, 0.5 g of mango fruit pulp was homogenized with 20 mL of a methanol (Chem-Lab., Zedelgem, Belgium) solution in a dark glass bottle at room temperature. One mL of Folin–Ciocalteu’s reagent (LOBA Chemie PVT. Ltd., Mumbai, India) was mixed with 1 mL of the methanolic extract and reacted for 6 min at room temperature. Then, 4 mL of 1 M sodium carbonate (LOBA Chemie PVT. Ltd., Mumbai, India) and 3 mL water were added to the mixture. The samples were incubated for 90 min at room temperature in darkness, and the absorbance of the mixture was measured at 760 nm using a spectrophotometer (JENWAY, Model 6300, Staffordshire, UK). Total phenolic content was expressed as mg of gallic acid equivalent per g of fruit fresh weight.

2.7.9. Decay Percentage

Coated and uncontrol mango fruits were examined visually for decay symptoms. Fruits with any signs of microbial infection, i.e., brown spot, spoilage, or softened area,

was considered as decayed; the following equation (Equation (2)) calculated the decay percentage:

$$\text{Decay percentage} = (\text{number of decayed fruits} / \text{total number of fruits}) \times 100 \quad (2)$$

2.8. Statistical Analysis

The experiment was carried out in a complete randomized design (CRD) with three replicates. The experimental data were subjected to analysis of variance (ANOVA) to determine the effect of coating treatments on fruit quality parameters at each sampling time during storage. The statistical analysis was performed using R software, version 4.0.5, R Core Team, Vienna, Austria [44]. Significant differences among treatments ($p \leq 0.05$) were assessed by means of multiple Duncan range tests.

3. Results and Discussion

3.1. Particle Size and Zeta Potential

The Dynamic Light Scattering (DLS) results were obtained for ZnO NPs with an average size of 245.2 nm (Figure 1A), indicating particle aggregation in the solutions.

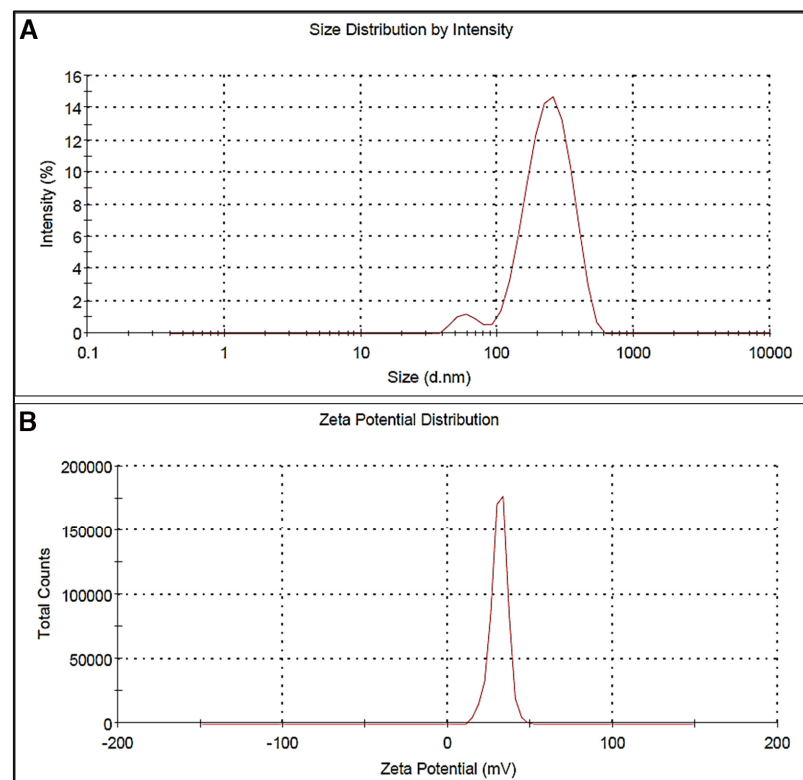


Figure 1. DLS analyses of ZnO NPs (A) and zeta potential (B).

The stability of the suspension can be monitored by measuring the zeta potential of the ZnO NPs, which was 31 mV (Figure 1B). A zeta potential value of ± 30 mV is generally chosen to deduce particle stability, with an absolute value greater than 30 mV designated as a stable condition [45,46].

3.2. Transmission Electron Microscopy (TEM) of ZnO NPs

Transmission electron microscopy (TEM) analysis was carried out on the ZnO NPs to obtain high accuracy images of the actual particle size and shape. The morphology of the ZnO NPs showed a spherical shape with some agglomerated particles (Figure 2). It can be seen from the image that the ZnO NP sizes ranged from 12 to 15.1 nm. Rasha et al. [47] documented similar observations.

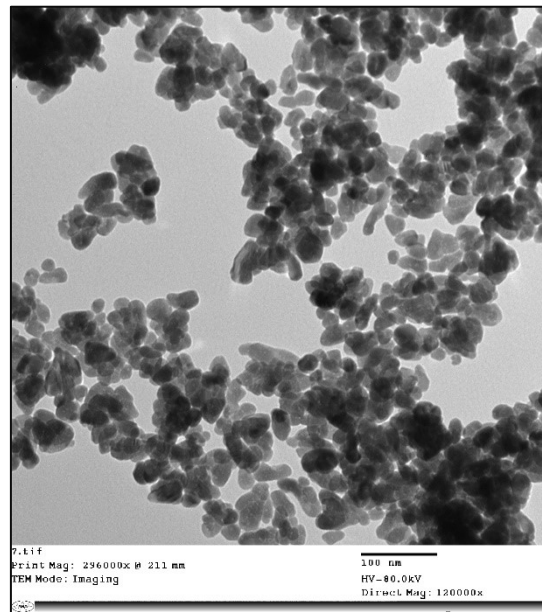


Figure 2. Transmission electron microscopy (TEM) micrograph of ZnO NPs.

3.3. Scanning Electron Microscopy (SEM) and Energy-Dispersive X-ray Spectroscopy (EDX) of ZnO NPs

The Scanning Electron Microscopy (SEM) analyses determined the surface morphology of ZnO NPs (Figure 3). The micrographs of the synthesized ZnO NPs display many agglomerated particles with irregular spherical shapes. This agglomeration is due to the polarity and electrostatic attraction of ZnO NPs nanoparticles. These results were confirmed by Fakhari et al. [48] and Umar et al. [49].

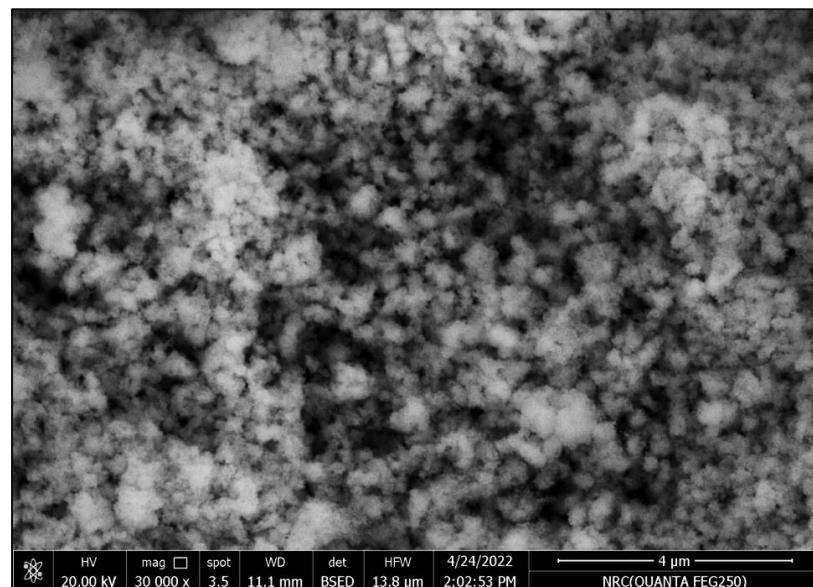


Figure 3. Scanning electron microscope (SEM) micrograph of ZnO NPs.

The elemental composition of the ZnO NPs was determined via energy-dispersive X-ray spectroscopy (EDX) analysis (Figure 4). The EDX spectrum revealed that the nanoparticles were composed of two elements, Zn and O, with mass percentages of 82.48% and 17.52%, respectively (Table 1). This result confirmed the high purity for the synthesized ZnO NPs. A similar finding was also found in previous studies by Rasha et al. [47], Fakhari et al. [48], and Hasnidawani et al. [50].

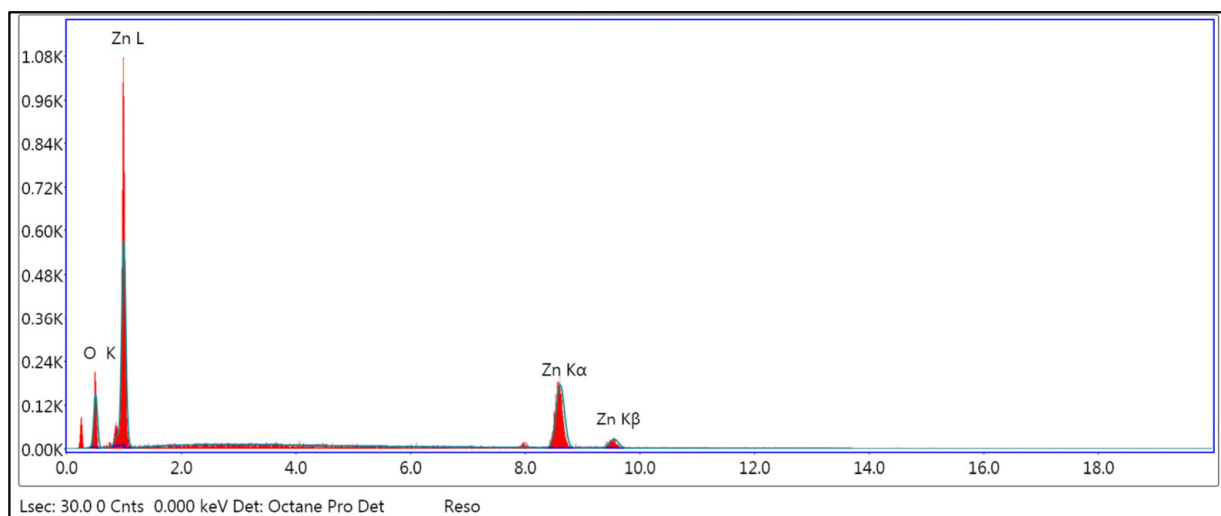


Figure 4. Energy-dispersive X-ray spectroscopy (EDX) of ZnO NPs.

Table 1. Elemental analysis of energy-dispersive X-ray spectroscopy (EDX).

Element	Weight %	Atomic %
O K	17.52	46.46
Zn K	82.48	53.54

3.4. Fourier-Transform Infrared Spectroscopy

Figure 5 shows the FTIR spectra of the zinc acetate and ZnO NPs. The characteristic absorbance bands observed at 1548 and 1434 cm^{-1} can be assigned to the COO[−] stretching vibrations in the FTIR spectrum of zinc acetate and the peaks at 1057 and 1016 cm^{-1} indicate the lattice vibration of carbonate-generated absorption (Figure 5A), which disappeared in the FTIR spectrum of the ZnO NPs [51–53]. A sharp peak was observed at 3073 cm^{-1} due to the bending vibration and the stretching vibration of O–H, corresponding to dehydration of zinc acetate. This band was reduced, and a wide band was formed in the ZnO NP spectrum at 3357 cm^{-1} (Figure 5B). The peaks at 529, 432, and 415 cm^{-1} are attributed to Zn–O stretching and deformation vibrations, which confirmed the formation of ZnO NPs (Figure 5B). Metal oxides generally give absorption peaks between 600 and 400 cm^{-1} [54,55].

3.5. Antimicrobial Properties of Alg–ZnO NPs

The Gram-negative bacteria *E. coli* and Gram-positive bacteria *S. aureus* were used to investigate the antibacterial activities of alginate-based ZnO NPs (Alg–ZnO NPs) compared to the polymyxin antibiotic (control). The antibacterial activity was investigated using Mueller–Hinton agar medium and the agar well diffusion assay. The difference between the inhibition zones is illustrated in Figure 6. Alg–ZnO NPs showed similar antibacterial activity against both *E. coli* and *S. aureus*. However, the control had a significantly larger inhibition zone against *S. aureus* compared to that against *E. coli*. The differences in sensitivity to Gram-positive bacteria compared to Gram-negative bacteria have been reported previously [56,57].

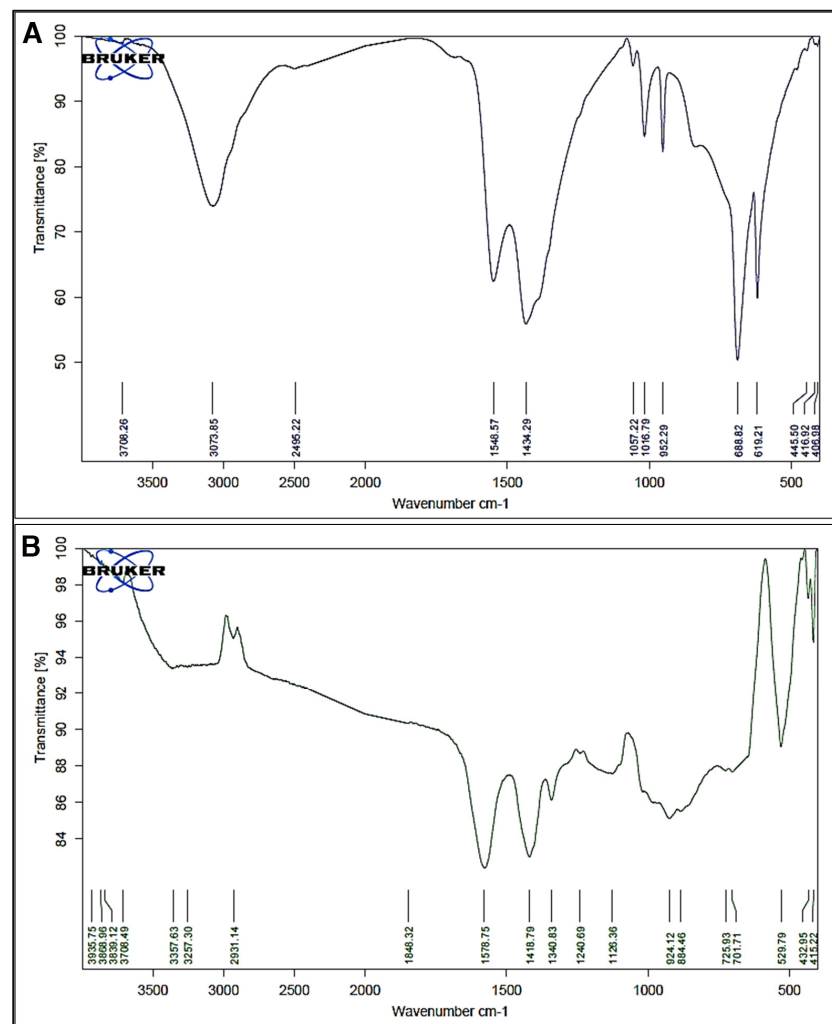


Figure 5. FTIR spectrum of (A) zinc acetate; (B) ZnO NPs.

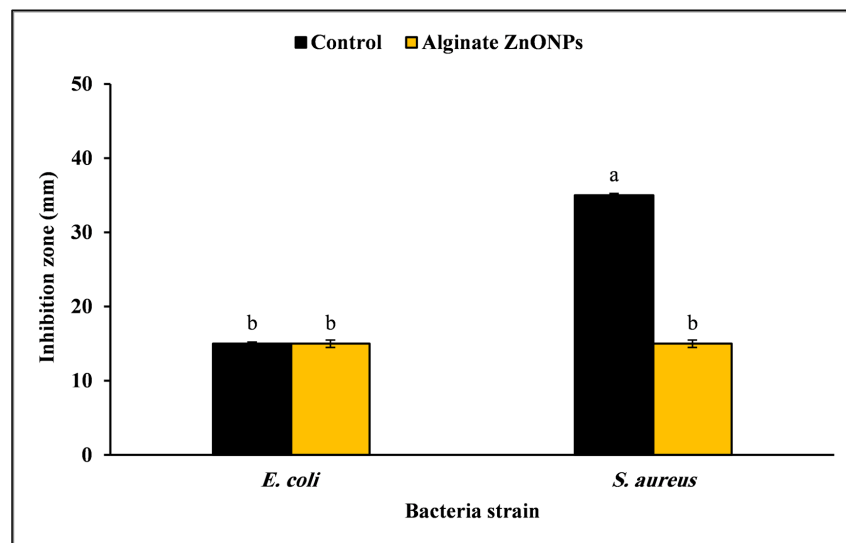


Figure 6. Inhibition zone diameter (mm) of Alg-ZnO NPs against *Escherichia coli* and *Staphylococcus aureus* compared to control (polymyxin antibiotic) using well diffusion method; vertical bars represent the standard error (SE). Bars marked with the same letter are not significantly different with 95% confidence according to Duncan's multiple range test.

Previous work has documented the antibacterial activity of ZnO NPs against various bacteria including *E. coli* [58] and *S. aureus* [59]. The potential mechanism involved in the antibacterial activity may be related to the generation of reactive oxygen species (ROS), which can damage bacterial proteins, DNA, and lipids, disturb the cellular systems, and consequently result in growth inhibition and cell death [29,60,61]. Moreover, ZnO NPs can inhibit the metabolism of amino acids and disrupt enzyme activity [28].

3.6. Fruit Quality Assessment

3.6.1. Respiration Rate

The change in the respiration rate of mango fruits during the storage period is represented in Figure 7. A significant increase in respiration rate ($p \leq 0.05$) was recorded during the storage period of both coated and uncoated fruits. However, the lowest respiration rate was observed in Alg–ZnO NP-coated fruits, followed by the fruit coated with alginate, while the highest respiration rate was recorded with uncoated fruits (control). The respiration rates of the control and coated fruits were low during the first 14 days of storage; afterwards, they exhibited a sharp increase (Figure 7). The respiration rate in the controls was significantly ($p \leq 0.05$) and consistently more remarkable than the coated fruits across the entirety of the storage period.

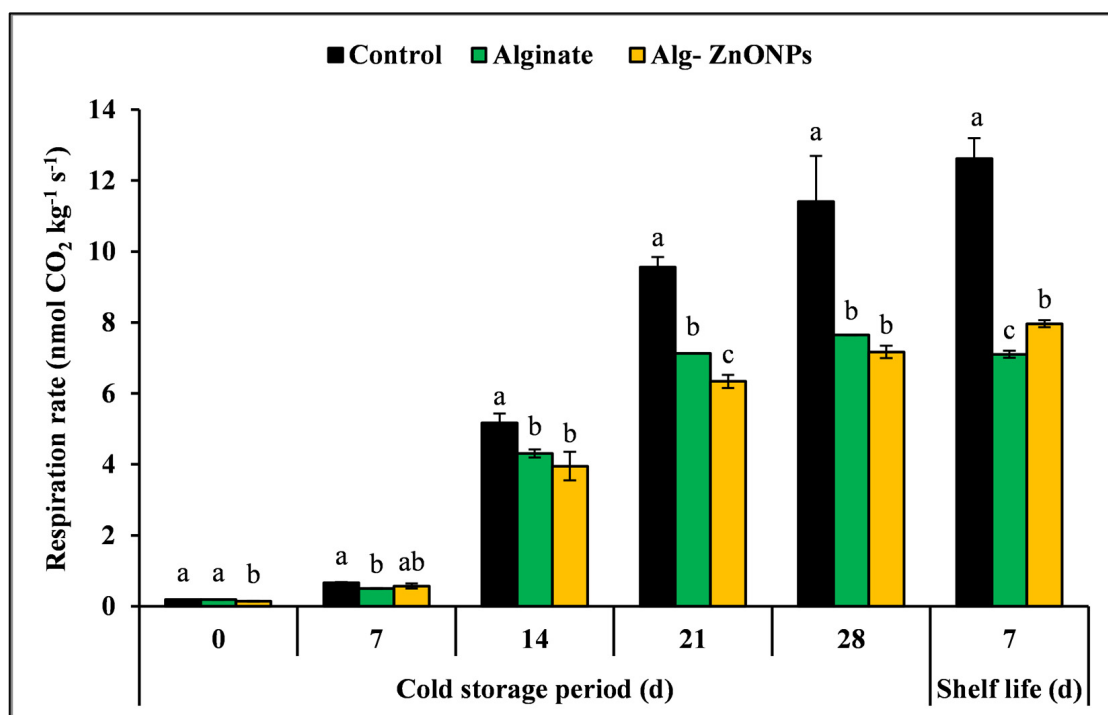


Figure 7. Effect of Alg–ZnO NPs on respiration rate of “Kiett” mango fruits during cold storage and shelf life; vertical bars represent the standard error (SE). Bars marked with the same letter in each sampling date are not significantly different with 95% confidence according to Duncan’s multiple range test.

The ripening of climacteric fruits such as mango is characterized by a significant and rapid increase in respiration rate accompanied by intensive metabolic changes [62]. The coating materials operate as a semi-permeable barrier to the exchange of gases and movement of solvents and moisture, thus decelerating the rate of respiration [63]; hence, uncoated fruits showed faster perishable behavior than coated fruits. ZnO NPs significantly improved the water vapor barrier and mechanical properties of the edible coatings [64,65], enriching carboxymethyl cellulose with ZnO NPs reduced the respiration rate during tomato fruit storage [66]. Moreover, chitosan coatings incorporating ZnO NPs restricted fresh-cut kiwifruit gas exchange [67].

3.6.2. Weight Loss

It was clearly observed that the mango fruit weight loss (WL) progressively increased in all treatments over the storage period, as shown in Figure 8.

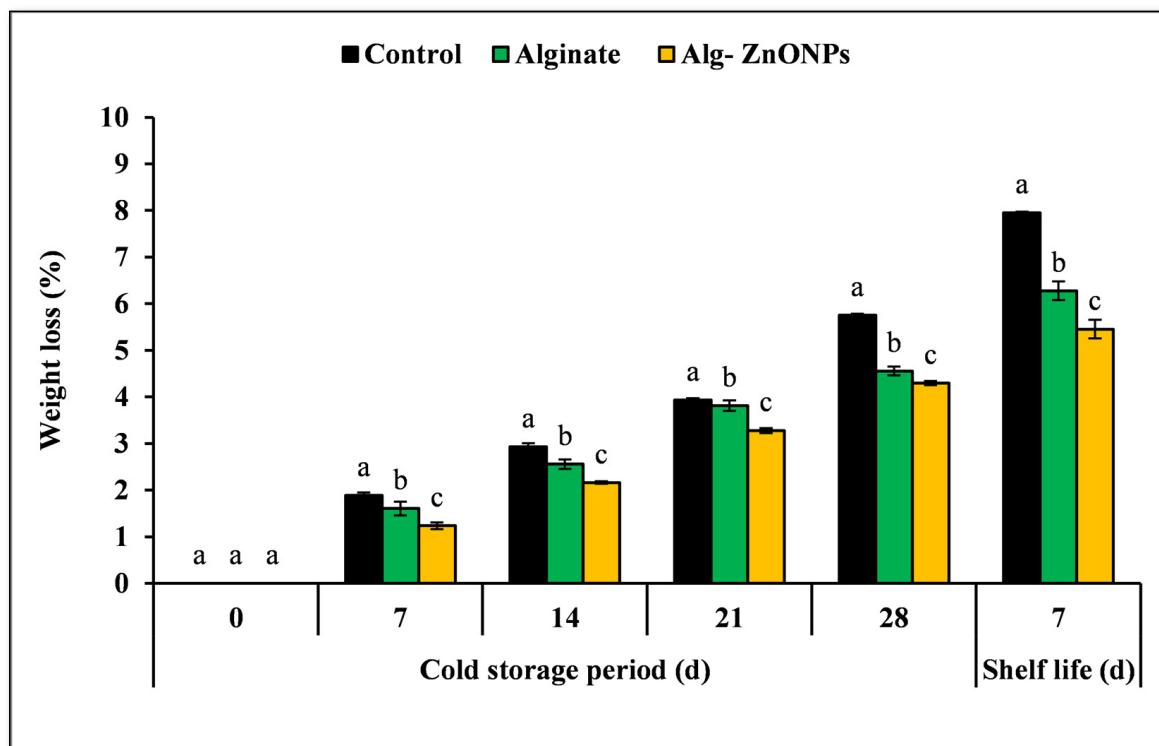


Figure 8. Effect of Alg–ZnO NPs on weight loss of “Kiett” mango fruits during cold storage and shelf life; vertical bars represent the standard error (SE). Bars marked with the same letter in each sampling date are not significantly different with 95% confidence according to Duncan’s multiple range test.

However, compared with the control treatment, the coatings efficiently slowed down the weight loss rate during storage, particularly with Alg–ZnO NP and alginate coating treatments. Mango fruits in the uncoated group displayed higher WL (5.75%) after 28 days of storage at 13 °C, while on the same date, the weight loss values of the fruits coated with Alg–ZnO NPs and alginate were 4.30% and 4.56%, respectively. Water loss during storage results in reduced fruit weight, shrinkage, and decreased postharvest quality value of fresh fruits [68]. The reduction in weight loss in the coated samples with biopolymer-based edible coatings was reported previously in a wide range of fruit crops [13,32,36,69,70]. Climacteric mature fruit undergoes a series of metabolic changes when detached from the tree, and these metabolic processes eventually result in fruit weight loss during the postharvest and storage period [62,71]. The coating material can mitigate the loss of water and reduce these deleterious effects; coating acts as a semi-permeable barrier for moisture, oxygen, and carbon dioxide, thereby reducing respiration and water loss and maintaining the turgescence of cell walls [72]. Wu et al. [73] found that adding ZnO NPs to polysaccharide-based biopolymers significantly improved their mechanical properties and reduced water vapor permeability. According to Emamifar and Bavaisi [74], ZnO NPs significantly increased the moisture barrier of alginate films, therefore reducing fruit weight loss.

3.6.3. Fruit Pulp Firmness

Fruit pulp firmness was found to be gradually decrease for all treatments over the storage period (Figure 9). Notably, the coating treatments maintained higher firmness and postponed the loss of fruit texture; the maximum loss of firmness was found at the end

of the storage period in the control fruits, while the firmness of mango fruits coated with Alg-ZnO NPs was significantly ($p \leq 0.05$) higher than those of the control group during the whole storage period; at the end of the storage period, the firmness of non-coated, alginate- and Alg-ZnO NP-coated fruits declined to 14.17 N, 17.53 N, and 22.65 N, respectively. Fruit pulp firmness is a vital aspect of fresh fruit quality, and maintenance of mango fruit firmness is fundamental for fruit handling, transport, and storage [75]. Firmness loss is explained as a loss of cellular turgidity and degradation of the middle lamella between cells by enzyme activity including the hydrolysis of polysaccharides within the fruit cells during ripening [9,76]. Starch, pectin, and hemicelluloses are major cell wall polysaccharides that decrease during fruit ripening [9]. The maintenance of the pulp firmness of the coated fruits may be attributed to reduced respiration and other ripening processes during storage. This could be explained by the fact that coating restricted gas exchange, reducing enzyme activity and leading to textural softening. The coating material effectively slowed down the metabolic and enzymatic activities in the fruits, resulting in the slower degradation of pulp tissues [67].

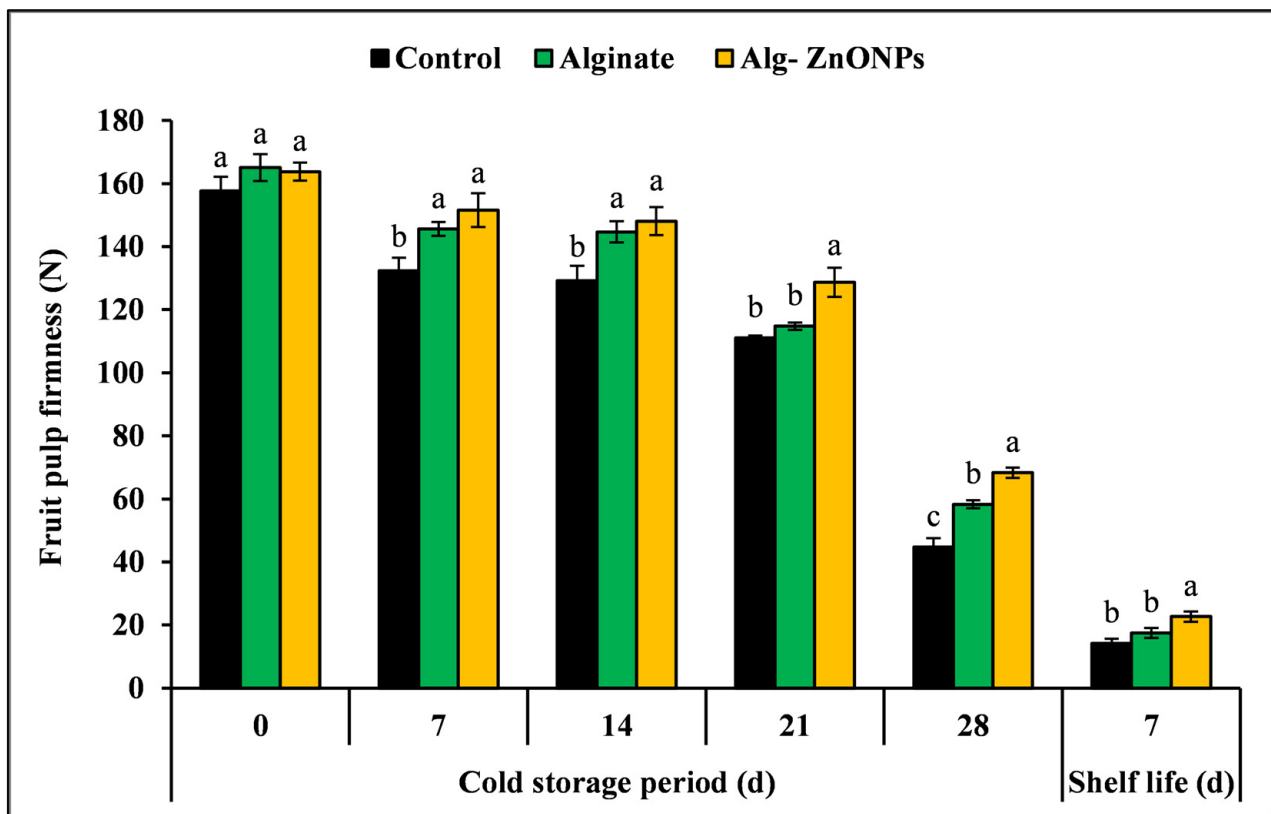


Figure 9. Effect of Alg-ZnO NPs on pulp firmness of “Kiett” mango fruits during cold storage and shelf life; vertical bars represent the standard error (SE). Bars marked with the same letter in each sampling date are not significantly different with 95% confidence according to Duncan’s multiple range test.

3.6.4. Total Soluble Solids (TSS), Titratable Acidity (TA), and TSS/TA Ratio

The results showed that the total soluble solid content of mango pulp underwent a gradual increase during the storage period in all treatments (Figure 10).

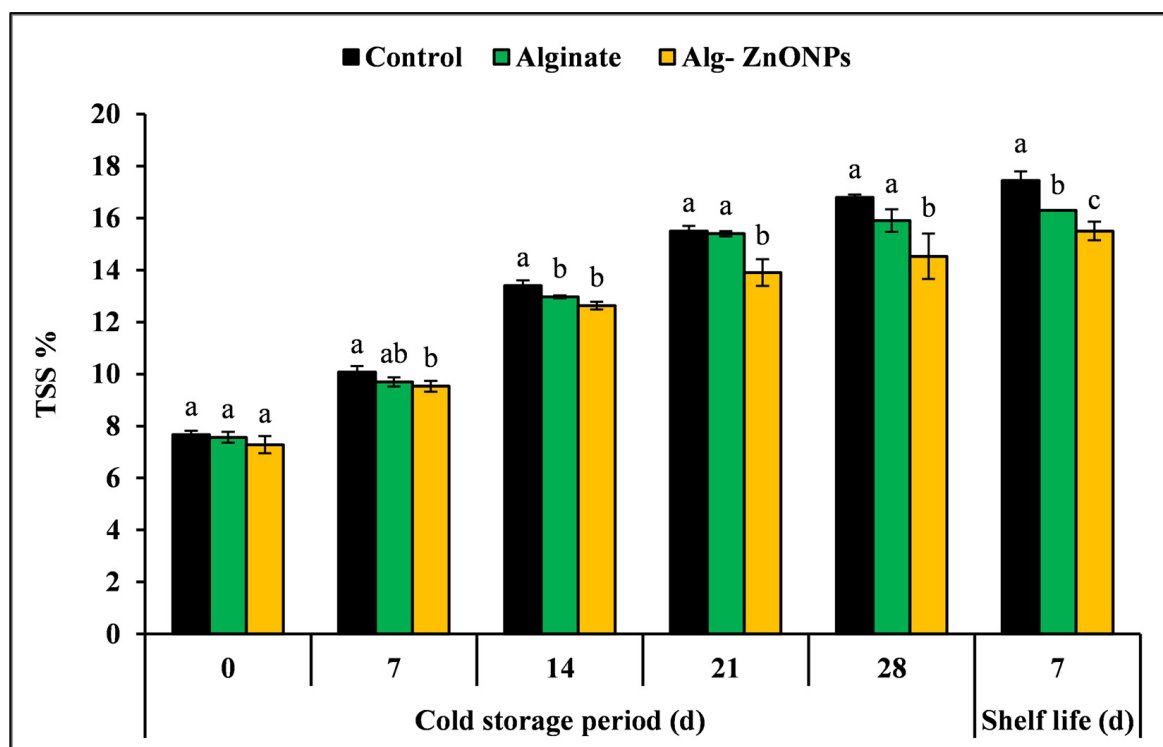


Figure 10. Effect of Alg–ZnO NPs on total soluble solids (TSS) of “Kielt” mango fruits during cold storage and shelf life; vertical bars represent the standard error (SE). Bar marked with the same letter in each sampling date are not significantly different with 95% confidence according to Duncan’s multiple range test.

Statistically significant variations were observed in the TSS content between the coating treatments at different sampling times during storage. The increase was significantly ($p \leq 0.05$) lower in coated fruits than in control. Fruits coated with Alg–ZnO NPs had lower TSS values than alginate coatings during storage. The maximum TSS after 28 days of storage was recorded as 16.80° Brix in the controls, whereas it was recorded as 15.90 and 14.53 in the alginate and Alg–ZnO NP treatments, respectively (Figure 10). During the storage period, the variations in TSS could be due to the hydrolysis of complex carbohydrates by the activities of hydrolytic enzymes [70]. In previous studies on coated fruits, similar findings were also observed regarding the effect of coatings in decelerating the increase in TSS [32,72,77]. Gol et al. [78] suggested that the low TSS for coated fruits presumably occurred because of the barrier effect of the coating against respiration, thus decelerating the metabolic activities of the fruits.

The result of the different coating treatments on titratable acidity (TA) values of the mango fruits during the storage period is shown in Figure 11. A general gradual decline was detected in the TA for all treatments over the storage period. The results of the TA illustrated that the coatings reduced the trend for TA decline in mango fruits compared to the control during the storage period. The results indicated that the TA of all samples significantly ($p \leq 0.05$) declined from (10.35 to 11.31%) at the beginning of the storage period to 2.56, 3.79, and 4.48 for uncoated, alginate, and Alg–ZnO NP treatments, respectively. The decline in fruit acidity during fruit ripening is associated with a reduction in organic acids, which are the primary substrates for the respiration process of climatic fruits [79]. In other words, as mentioned earlier, the application of coatings decelerates the rate of respiration and metabolic processes, thus limiting the excess intake of organic acids in respiration reactions [19,20]. Compared with the uncoated fruit samples, the edible coating has been proven to efficiently slow the fruit respiration rate, thus inhibiting the consumption of titratable acids [80].

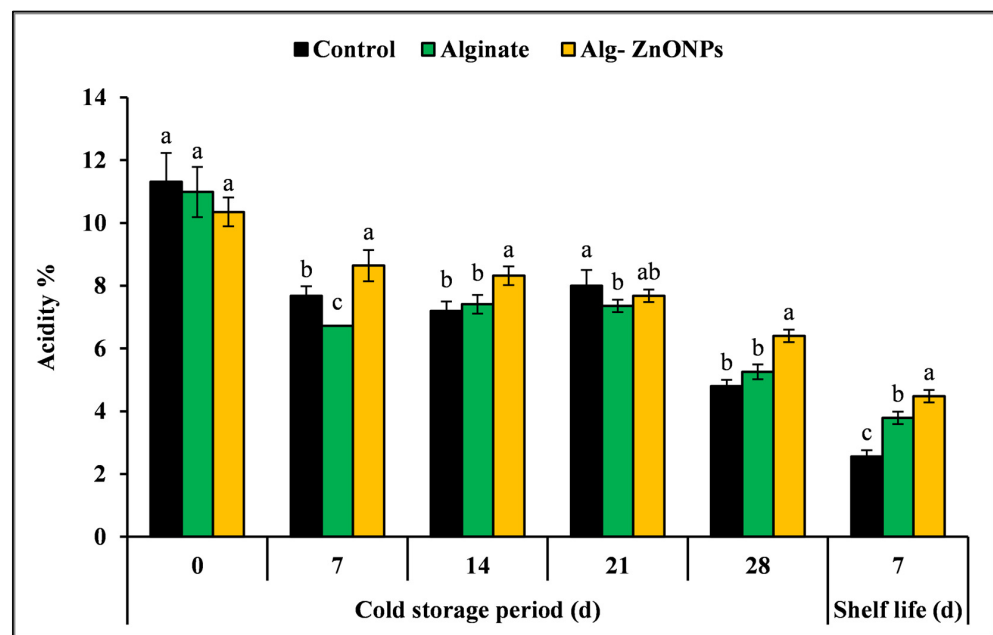


Figure 11. Effect of Alg-ZnO NPs on titratable acidity (TA) of “Kiett” mango fruits during cold storage and shelf life; vertical bars represent the standard error (SE). Bars marked with the same letter in each sampling date are not significantly different with 95% confidence according to Duncan’s multiple range test.

The TSS/TA ratio was significantly affected by the coating treatments during the storage period. The TSS/TA ratio values for the coated fruits were lower than those of the uncoated fruits (Figure 12).

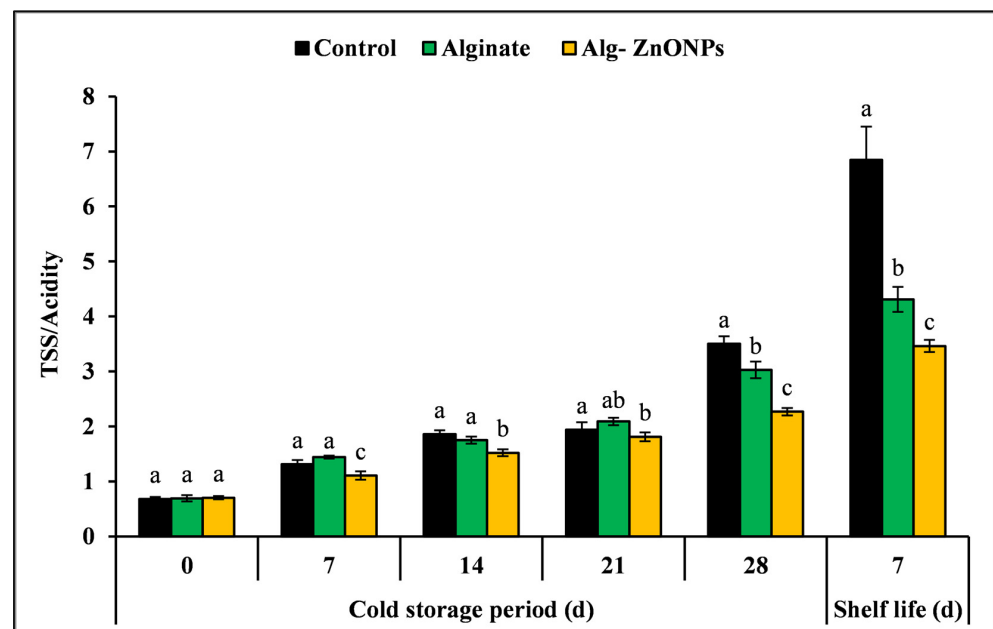


Figure 12. Effect of Alg-ZnO NPs on TSS/TA ratio of “Kiett” mango fruits during cold storage and shelf life; vertical bars represent the standard error (SE). Bars marked with the same letter in each sampling date are not significantly different with 95% confidence according to Duncan’s multiple range test.

A non-significant difference was observed between alginate and Alg-ZnO NP coatings during the storage period up to 21 days. The TSS/TA ratio showed a rapid increase in

uncoated fruits, indicating increased fruit ripening rate. The ratio of TSS/TA is known to be an indicator of fruit quality; the sweet taste is the result of increased hydrolysis of polysaccharides (mainly starch), decreased acidity, and accumulation of sugars, which results in an excellent sugar/acid ratio [9].

3.6.5. Total and Reducing Sugar Content

The increase in soluble sugars during ripening provides a sweet taste to the mango fruit; total and reducing sugar values for the different samples were initially recorded at 91.55 and 44.94 mg g⁻¹, respectively. The total and reducing sugar content of all treatments increased consistently during the storage period (Figure 13A,B). Total sugar content increased slower in coated fruits, while a sharp increase was observed in uncoated fruits during the whole storage period. The soluble sugar content of the uncoated and coated fruits differed slightly until 14 days, while Alg-ZnO NP-coated fruits recorded the lowest total and reduced sugar content during the whole storage period. The accumulation of sugars increased with fruit ripening due to the hydrolysis of polysaccharides leading to the production of soluble sugars during storage [9,81]; soluble sugars in ripe fruits mainly consist of glucose, fructose, and sucrose [82]. The coating inhibits the transition of complex carbohydrates into simple sugars [32]. The rapid change in total sugars of the control treatment can be explained by the mango fruit respiratory burst, which is distinguished by significant changes in fruit biochemical activity leading to fruit ripening [83]. Silva et al. [68] highlighted that the fruit coating treatments reduce respiratory activity and ethylene production, which slow the ripening process, delay the climacteric peak, and increase fruit storage life.

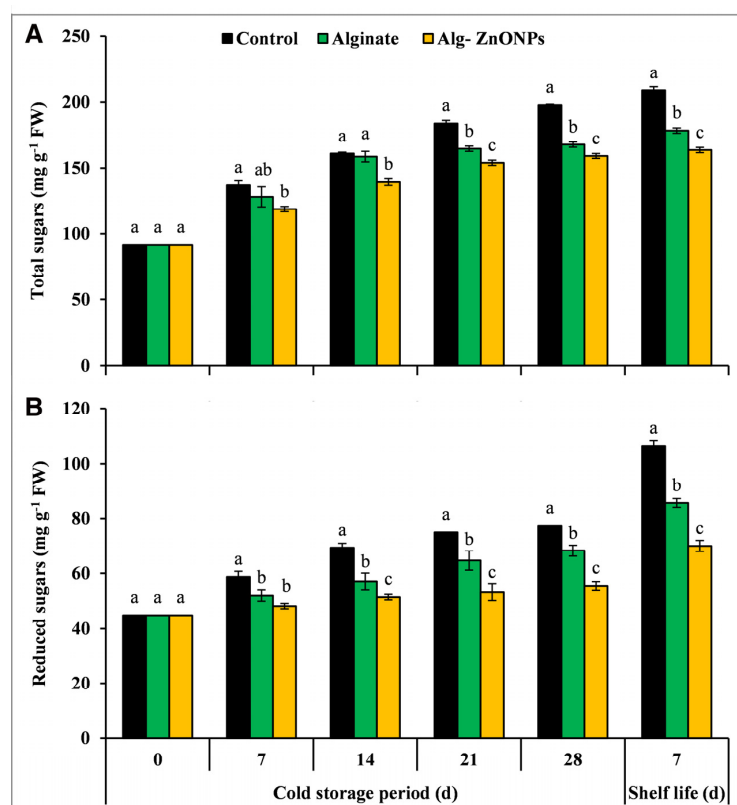


Figure 13. Effect of Alg-ZnO NPs on total sugars (A) and reducing sugars (B) of “Kiatt” mango fruits during cold storage and shelf life; vertical bars represent the standard error (SE). Bars marked with the same letter in each sampling date are not significantly different with 95% confidence according to Duncan’s multiple range test.

3.6.6. Total Carotenoids Content

Color changes in mango fruits are due to the disappearance of chlorophyll and the appearance of other pigments. As ripening progressed in all fruits, a steady increase in carotenoid content was noted, but the rate was slower in coated fruits (Figure 14).

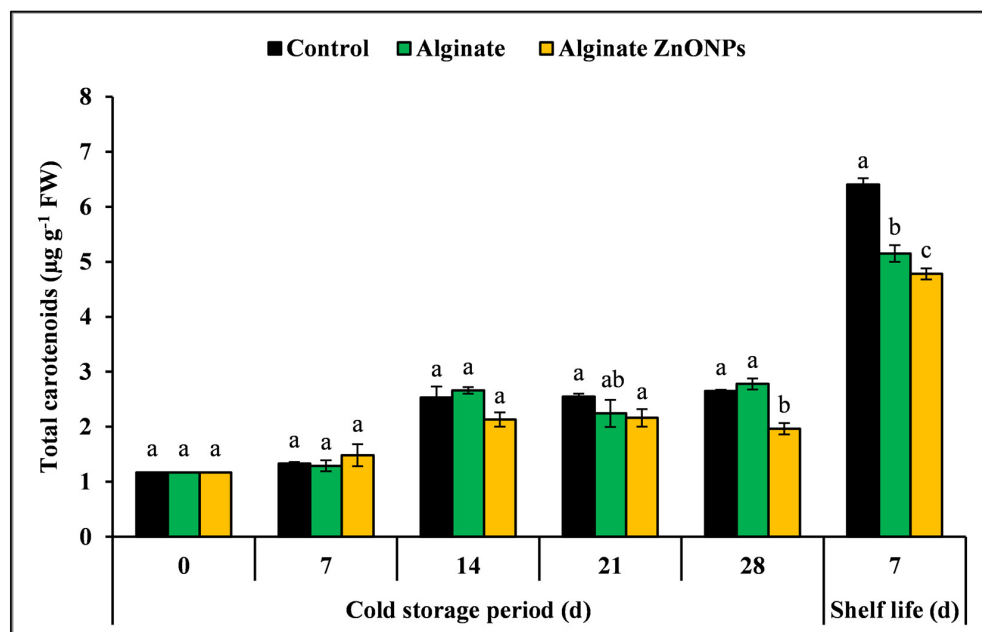


Figure 14. Effect of Alg–ZnO NPs on total carotenoids of “Kielt” mango fruits during cold storage and shelf life; vertical bars represent the standard error (SE). Bars marked with the same letter in each sampling date are not significantly different with 95% confidence according to Duncan’s multiple range test.

Statistical analysis showed that the differences ($p \leq 0.05$) between the coating treatments were slight and insignificant until day 21 of storage; afterwards, the carotenoid content was significantly lower for fruits coated Alg–ZnO NPs. The Alg–ZnO NPs coating seemed to delay the accumulation of carotenoids more than the alginate coating. The control mangoes showed the highest carotenoid content ($6.41 \mu\text{g g}^{-1}$) after five weeks of storage. The delay in the ripening and internal color development of the coated fruit can be attributable to the limited respiration rate of the coated fruit, which decreases chlorophyll degradation and/or carotenoid biosynthesis [13]. Polysaccharide-based composite coatings have synergistic effects on color retention by delaying the development of coloring pigments in mango fruits [70].

3.6.7. Total Phenol Content

Phenolic compound contents declined in both coated and uncoated mango fruits during the storage period and, subsequently, shelf life (Figure 15). Although the declining rate was more evident in the control fruit, the total phenol reduced during five weeks from 7.22 to 0.71 , 3.25 , and 3.55 mg g^{-1} in the control, alginate-, and Alg–ZnO NP-coated fruits, respectively. At the end of the experiment, coated fruits maintained higher phenolic contents than the control. Previous studies showed a lower rate of phenolic compound degradation in coated mango fruits [84]. Phenolic compounds affect fruit quality parameters, i.e., fruit taste, flavor, and aroma, and capture reactive oxygen species that are produced during fruit ripening [85]; the alginate coating preserved the phenolic content during the storage period by delaying fruit ripening [69] since edible coatings decrease gas exchange and reduce the degradation rates of phenols [16,63]. According to Emamifar and Bavaisi [74], adding ZnO NPs to sodium alginate coatings decreases gas exchange and hence reduces enzymatic oxidation of phenolic compounds.

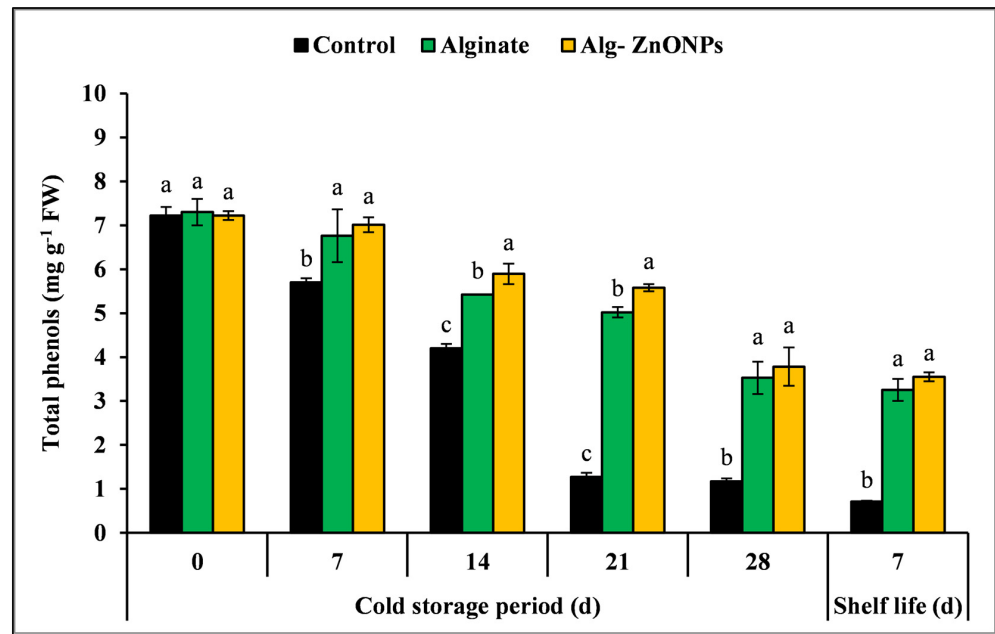


Figure 15. Effect of Alg-ZnO NPs on total phenols of “Kiett” mango fruits during cold storage and shelf life; vertical bars represent the standard error (SE). Bars marked with the same letter in each sampling date are not significantly different with 95% confidence according to Duncan’s multiple range test.

3.6.8. Decay Percentage

The data summarized in Figure 16 shows the values of decay incidence in both coated and uncoated mango fruits (control); there were no visible signs of decay in the stored mango fruits during the entire storage period (28 days).

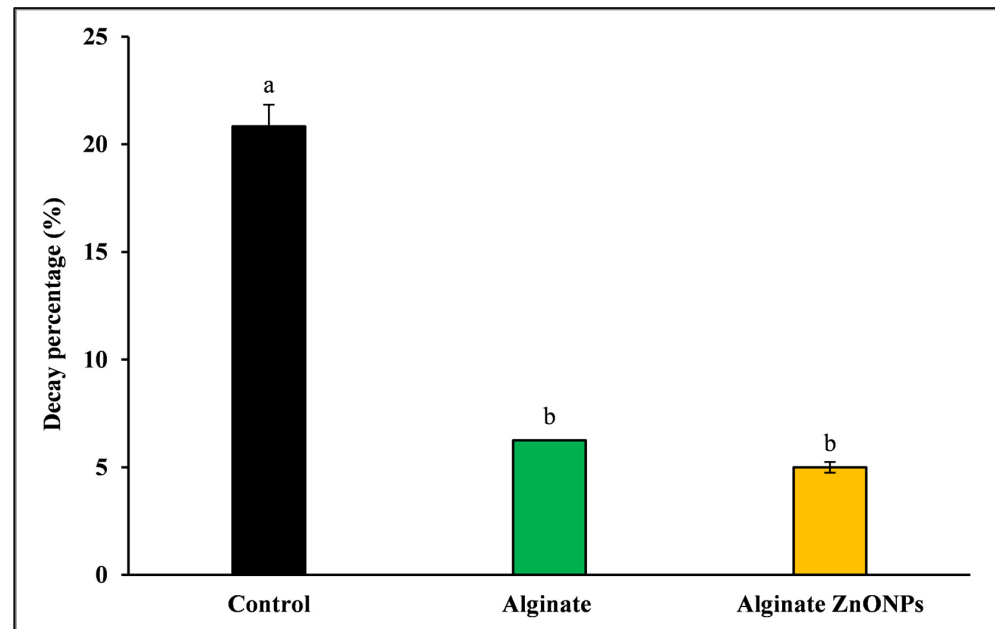


Figure 16. Effect of Alg-ZnO NPs on decay percentage of “Kiett” mango fruits during shelf life period; vertical bars represent the standard error (SE). Bars marked with the same letter are not significantly different with 95% confidence according to Duncan’s multiple range test.

During the shelf life, the coating treatments significantly ($p \leq 0.05$) reduced the decay percentage compared to the control treatment. The decay percentage of the control

treatment was approximately three to four times higher than that of alginate- and Alg–ZnO NP-coated fruits, respectively. The decrease in decay incidence was probably due to the effect of the coating on delaying senescence, which results in lower pathogenic infections [86]. Moreover, ZnO NPs have anti-microbial effects against the activity of several postharvest microbial infections [56,57]. The obtained results confirm the anti-microbial properties of Alg–ZnO NPs.

4. Conclusions

The Alg–ZnO NP coating treatment can effectively improve fruit quality parameters such as reducing weight loss, respiration rate, maintaining firmness, and reducing microbial decay of mango fruits ‘cv. Kiett’. The increases in the rate of total soluble solids, total sugars, and carotenoids in the coated fruits were controlled and slowed down. These results suggest that coatings loaded with synthesized ZnO NPs can be efficiently used to retard the ripening and prolong the postharvest life of mango fruits. The findings of this research may be applied to improving the postharvest, storage, and marketing of mango fruits, which should lead to a rise in exports.

Author Contributions: Conceptualization, I.H.; methodology, M.A.-S.A. and A.A.; software, I.H. and M.A.-S.A.; validation, M.A.-S.A. and A.A.; formal analysis, I.H.; investigation, I.H., M.A.-S.A. and A.A.; resources, I.H., M.A.-S.A. and A.A.; data curation, A.A.; writing—original draft preparation, M.A.-S.A. and A.A.; writing—review and editing, I.H., M.A.-S.A. and A.A.; visualization, I.H.; supervision, I.H.; project administration, I.H.; funding acquisition, I.H. All authors have read and agreed to the published version of the manuscript.

Funding: This research was funded and supported by a research grant from the Science, Technology & Innovation Funding Authority (STIFA), under the grant STDF-YRG, No. 33528.

Institutional Review Board Statement: Not applicable.

Informed Consent Statement: Not applicable.

Data Availability Statement: Data are available upon request.

Acknowledgments: The authors would like to express special thanks to the Science and Technology Development Fund (STDF) (Current name: Science, Technology & Innovation Funding Authority (STIFA)) for funding and the Faculty of Agriculture, Cairo University for access to all facilities during this work. The authors would also like to extend their gratitude to their colleagues at the Department of Pomology, Faculty of Agriculture, Cairo University for their early assistance with the technical aspects of this work.

Conflicts of Interest: The authors declare no conflict of interest.

References

1. Singh, Z.; Singh, R.K.; Sane, V.A.; Nath, P. Mango-postharvest biology and biotechnology. *Crit. Rev. Plant Sci.* **2013**, *32*, 217–236. [[CrossRef](#)]
2. Jahurul, M.H.A.; Zaidul, I.S.M.; Ghafoor, K.; Al-Juhaimi, F.Y.; Nyam, K.L.; Norulaini, N.A.N.; Sahena, F.; Omar, A.M. Mango (*Mangifera indica* L.) by-products and their valuable components: A review. *Food Chem.* **2015**, *183*, 173–180. [[CrossRef](#)]
3. Sivakumar, D.; Jiang, Y.; Yahia, E.M. Maintaining mango (*Mangifera indica* L.) fruit quality during the export chain. *Food Res. Int.* **2011**, *44*, 1254–1263. [[CrossRef](#)]
4. Brecht, J.K.; Yahia, E.M. Postharvest Physiology. In *The Mango: Botany, Production and Uses*, 2nd ed.; Litz, R.E., Ed.; CAB International: Wallingford, UK, 2009; pp. 484–516.
5. Knight, R.J., Jr.; Campbell, R.J.; Maguire, I. Important Mango Cultivars and Their Descriptors. In *The Mango: Botany, Production and Uses*, 2nd ed.; Litz, R.E., Ed.; CAB International: Wallingford, UK, 2009; pp. 42–66.
6. Riad, M. Mango production in Egypt. *Acta Hortic.* **1997**, *1*, 1–6. [[CrossRef](#)]
7. Ntsoane, M.L.; Zude-Sasse, M.; Mahajan, P.; Sivakumar, D. Quality assesment and postharvest technology of mango: A review of its current status and future perspectives. *Sci. Hortic.* **2019**, *249*, 77–85. [[CrossRef](#)]
8. Sane, V.A.; Chourasia, A.; Nath, P. Softening in mango (*Mangifera indica* cv. Dashehari) is correlated with the expression of an early ethylene responsive, ripening related expansin gene, *MiExpA1*. *Postharvest Biol. Technol.* **2005**, *38*, 223–230. [[CrossRef](#)]

9. Cárdenas-Coronel, W.G.; Velez-de la Rocha, R.; Siller-Cepeda, J.H.; Osuna-Enciso, T.; Muy-Rangel, M.D.; Sañudo-Barajas, J.A. Changes in the composition of starch, pectin and hemicellulose during ripening of mango (*Mangifera indica* cv. Kent). *Rev. Chapingo Ser. Hortic.* **2012**, *18*, 5–19. [[CrossRef](#)]
10. Singh, Z.; Singh, S.P. Mango. In *Crop Post-Harvest: Science and Technology*; Rees, D., Orchard, J., Eds.; Blackwell Pub.: Perishables, UK, 2012; Volume 3, pp. 108–142.
11. Ridoutt, B.G.; Juliano, P.; Sanguansri, P.; Sellahewa, J. The water footprint of food waste: Case study of fresh mango in Australia. *J. Clean Prod.* **2010**, *18*, 1714–1721. [[CrossRef](#)]
12. Sheahan, M.; Barrett, C.B. Food loss and waste in Sub-Saharan Africa. *Food Policy* **2017**, *70*, 1–12. [[CrossRef](#)]
13. Carrillo-Lopez, A.; Ramirez-Bustamante, F.; Valdez-Torres, J.B.; Rojas-Villegas, R.; Yahia, E.M. Ripening and quality changes in mango fruit as affected by coating with an edible film. *J. Food Qual.* **2000**, *23*, 479–486. [[CrossRef](#)]
14. Parfitt, J.; Barthel, M.; Macnaughton, S. Food waste within food supply chains: Quantification and potential for change to 2050. *Philos. Transac-Tions R. Soc. Biol. Sci.* **2010**, *365*, 3065–3081. [[CrossRef](#)] [[PubMed](#)]
15. Nair, M.S.; Saxena, A.; Kaur, C. Effect of chitosan and alginate based coatings enriched with pomegranate peel extract to extend the postharvest quality of guava (*Psidiumguajava* L.). *Food Chem.* **2018**, *240*, 245–252. [[CrossRef](#)]
16. Hassan, B.; Chatha, S.A.S.; Hussain, A.I.; Zia, K.M.; Akhtar, N. Recent advances on polysaccharides, lipids and protein based edible films and coatings: A review. *Int. J. Biol. Macromol.* **2018**, *109*, 1095–1107. [[CrossRef](#)] [[PubMed](#)]
17. Maftoonazad, N.; Ramaswamy, H.S.; Marcotte, M. Shelf-life extension of peaches through sodium alginate and methyl cellulose edible coatings. *Int. J. Food Sci. Technol.* **2008**, *43*, 951–957. [[CrossRef](#)]
18. Dhall, R.K. Advances in edible coatings for fresh fruits and vegetables: A review. *Crit. Rev. Food Sci. Nutr.* **2013**, *53*, 435–450. [[CrossRef](#)]
19. Panahirad, S.; Naghshiband-Hassani, R.; Ghanbarzadeh, B.; Zaare-Nahandi, F.; Mahna, N. Shelf life quality of plum fruits (*Prunusdomestica* L.) improves with carboxymethylcellulose-based edible coating. *HortScience* **2019**, *54*, 505–510. [[CrossRef](#)]
20. Shah, S.; Hashmi, M.S. Chitosan–aloe vera gel coating delays postharvest decay of mango fruit. *Hortic. Environ. Biotechnol.* **2020**, *61*, 279–289. [[CrossRef](#)]
21. Qin, Y. Alginate fibres: An overview of the production processes and applications in wound management. *Polym. Int.* **2008**, *57*, 171–180. [[CrossRef](#)]
22. Cazón, P.; Velazquez, G.; Ramírez, J.A.; Vázquez, M. Polysaccharide-based films and coatings for food packaging: A review. *Food Hydrocoll.* **2017**, *68*, 136–148. [[CrossRef](#)]
23. Li, D.; Wei, Z.; Xue, C. Alginate-based delivery systems for food bioactive ingredients: An overview of recent advances and future trends. *Compr. Rev. Food Sci. Food Saf.* **2021**, *20*, 5345–5369. [[CrossRef](#)]
24. Vasilache, V.; Popa, C.; Filote, C.; Cretu, M.A.; Benta, M. Nanoparticles applications for improving the food safety and food processing. In Proceedings of the 7th International Conference on Materials Science and Engineering—BRAMAT, Bramat, Brasov, 24–26 February 2011; pp. 24–26.
25. Solaiman, M.A.; Ali, M.A.; Abdel-Moein, N.M.; Mahmoud, E.A. Synthesis of Ag-NPs developed by green-chemically method and evaluation of antioxidant activities and anti-inflammatory of synthesized nanoparticles against LPS-induced NO in RAW 264.7 macrophages. *Biocatal. Agric. Biotechnol.* **2020**, *29*, 101832. [[CrossRef](#)]
26. Abo-El-Yazid, Z.H.; Ahmed, O.K.; El-Tholoth, M.; Ali, M.A. Green synthesized silver nanoparticles using *Cyperus rotundus* L. extract as a potential antiviral agent against infectious laryngotracheitis and infectious bronchitis viruses in chickens. *Chem. Biol. Technol. Agric.* **2022**, *9*, 1–11. [[CrossRef](#)]
27. Ali, M.A.; Abdel-Moein, N.M.; Owis, A.S.; Ahmed, S.E.; Hanafy, E.A. Preparation, characterization, antioxidant and antimicrobial activities of lignin and eco-friendly lignin nanoparticles from Egyptian cotton stalks. *Egypt. J. Chem.* **2022**, *65*, 703–716. [[CrossRef](#)]
28. Kumar, R.; Umar, A.; Kumar, G.; Nalwa, H.S. Antimicrobial properties of ZnO nanomaterials: A review. *Ceram. Int.* **2017**, *43*, 3940–3961. [[CrossRef](#)]
29. Sun, Q.; Li, J.; Le, T. Zinc oxide nanoparticle as a novel class of antifungal agents: Current advances and future perspectives. *J. Agric. Food Chem.* **2018**, *66*, 11209–11220. [[CrossRef](#)] [[PubMed](#)]
30. Padmavathy, N.; Vijayaraghavan, R. Enhanced bioactivity of ZnO nanoparticles—An antimicrobial study. *Sci. Technol. Adv. Mate* **2008**, *3*, 035004. [[CrossRef](#)]
31. Gammariello, D.; Conte, A.; Buonocore, G.G.; Del Nobile, M.A. Bio-based nanocomposite coating to preserve quality of Fior di latte cheese. *J. Dairy Sci.* **2011**, *94*, 5298–5304. [[CrossRef](#)]
32. Hmam, I.; Zaid, N.M.; Mamdouh, B.; Abdallatif, A.; Abd-Elfattah, M.; Ali, M. Storage Behavior of “Seddik” mango fruit coated with CMC and guar gum-based silver nanoparticles. *Horticulturae* **2021**, *7*, 44. [[CrossRef](#)]
33. Bian, S.W.; Mudunkotuwa, I.A.; Rupasinghe, T.; Grassian, V.H. Aggregation and dissolution of 4 nm ZnO nanoparticles in aqueous environments: Influence of pH, ionic strength, size, and adsorption of humic acid. *Langmuir* **2011**, *27*, 6059–6068. [[CrossRef](#)]
34. Shamhari, N.M.; Wee, B.S.; Chin, S.F.; Kok, K.Y. Synthesis and characterization of zinc oxide nanoparticles with small particle size distribution. *Acta Chim. Slov.* **2018**, *65*, 578–585. [[CrossRef](#)]
35. Balouiri, M.; Sadiki, M.; Ibsnouda, S.K. Methods for *in vitro* evaluating antimicrobial activity: A review. *J. Pharm. Anal.* **2016**, *6*, 71–79. [[CrossRef](#)] [[PubMed](#)]

36. Iñiguez-Moreno, M.; Ragazzo-Sánchez, J.A.; Barros-Castillo, J.C.; Sandoval-Contreras, T.; Calderón-Santoyo, M. Sodium alginate coatings added with *Meyerozyma caribbica*: Postharvest biocontrol of *Colletotrichum gloeosporioides* in avocado (*Persea americana* Mill. cv. Hass). *Postharvest Biol. Technol.* **2020**, *163*, 111123. [CrossRef]
37. Tapia, M.S.; Rojas-Grau, M.A.; Carmona, A.; Rodriguez, F.J.; Soliva-Fortuny, R.; Martin-Belloso, O. Use of alginate- and gellan-based coatings for improving barrier, texture and nutritional properties of fresh-cut papaya. *Food Hydrocoll.* **2008**, *22*, 1493–1503. [CrossRef]
38. Pristijono, P.; Golding, J.B.; Bowyer, M.C. Postharvest UV-C treatment, followed by storage in a continuous low-level ethylene atmosphere, maintains the quality of ‘Kensington pride’ mango fruit stored at 20 °C. *Horticulturae* **2019**, *5*, 1. [CrossRef]
39. Liu, S.; Huang, H.; Huber, D.J.; Pan, Y.; Shi, X.; Zhang, Z. Delay of ripening and softening in ‘Guifei’ mango fruit by postharvest application of melatonin. *Postharvest Biol. Technol.* **2020**, *163*, 111136. [CrossRef]
40. Islam, M.; Khan, M.Z.H.; Sarkar, M.A.R.; Absar, N.; Sarkar, S.K. Changes in acidity, TSS, and sugar content at different storage periods of the postharvest mango (*Mangifera indica* L.) influenced by Bavistin DF. *Int. J. Food Sci.* **2013**, *2013*, 939385. [CrossRef] [PubMed]
41. Jain, A.; Jain, R.; Jain, S. Quantitative Analysis of Reducing Sugars by 3, 5-Dinitrosalicylic Acid (DNSA Method). In *Basic Techniques in Biochemistry, Microbiology and Molecular Biology*; Springer Protocols Handbooks; Humana: New York, NY, USA, 2020; pp. 181–183. [CrossRef]
42. Nielsen, S.S. Total Carbohydrate by Phenol-Sulfuric Acid Method. In *Food Analysis Laboratory Manual*; Food Science Text Series; Springer: Cham, Switzerland, 2017; pp. 137–141. [CrossRef]
43. Bärlocher, F.; Graça, M.A.S. Total Phenolics. In *Methods to Study Litter Decomposition*; Bärlocher, F., Gessner, M., Graça, M., Eds.; Springer: Cham, Switzerland, 2020; pp. 157–161. [CrossRef]
44. R Core Team. *R: A Language and Environment for Statistical Computing*; R Foundation for Statistical Computing: Vienna, Austria, 2021; Available online: <https://www.R-project.org/> (accessed on 19 January 2023).
45. Suganthi, K.S.; Rajan, K.S. Temperature induced changes in ZnO–water nanofluid: Zeta potential, size distribution and viscosity profiles. *Int. J. Heat Mass Transf.* **2012**, *55*, 7969–7980. [CrossRef]
46. Sapsford, K.E.; Tyner, K.M.; Dair, B.J.; Deschamps, J.R.; Medintz, I.L. Analyzing nanomaterial bioconjugates: A review of current and emerging purification and characterization techniques. *Anal. Chem.* **2011**, *83*, 4453–4488. [CrossRef]
47. Rasha, E.; Monerah, A.; Manal, A.; Rehab, A.; Mohammed, D.; Doaa, E. Biosynthesis of Zinc Oxide Nanoparticles from *Acacia nilotica* (L.) Extract to Overcome Carbapenem-Resistant *Klebsiella Pneumoniae*. *Molecules* **2021**, *26*, 1919. [CrossRef]
48. Fakhari, S.; Jamzad, M.; Kabiri Fard, H. Green synthesis of zinc oxide nanoparticles: A comparison. *Green Chem. Lett. Rev.* **2019**, *12*, 19–24. [CrossRef]
49. Umar, H.; Kavaz, D.; Rizaner, N. Biosynthesis of zinc oxide nanoparticles using *Albizia lebbek* stem bark, and evaluation of its antimicrobial, antioxidant, and cytotoxic activities on human breast cancer cell lines. *Int. J. Nanomed.* **2019**, *14*, 87–100. [CrossRef] [PubMed]
50. Hasnidawani, J.N.; Azlina, H.N.; Norita, H.; Bonnia, N.N.; Ratim, S.; Ali, E.S. Synthesis of ZnO nanostructures using sol-gel method. *Procedia Chem.* **2016**, *19*, 211–216. [CrossRef]
51. Choy, J.H.; Kwon, Y.M.; Han, K.S.; Song, S.W.; Chang, S.H. Intra-and inter-layer structures of layered hydroxy double salts, $\text{Ni}_{1-x}\text{Zn}_{2x}(\text{OH})_2(\text{CH}_3\text{CO}_2)_{2x}n\text{H}_2\text{O}$. *Mater. Lett.* **1998**, *34*, 356–363. [CrossRef]
52. Sakohara, S.; Ishida, M.; Anderson, M.A. Visible luminescence and surface properties of nanosized ZnO colloids prepared by hydrolyzing zinc acetate. *J. Phys. Chem. B* **1998**, *102*, 10169–10175. [CrossRef]
53. Wu, C.M.; Baltrusaitis, J.; Gillan, E.G.; Grassian, V.H. Sulfur dioxide adsorption on ZnO nanoparticles and nanorods. *J. Phys. Chem. C* **2011**, *115*, 10164–10172. [CrossRef]
54. Singh, R.P.; Shukla, V.K.; Yadav, R.S.; Sharma, P.K.; Singh, P.K.; Pandey, A.C. Biological approach of zinc oxide nanoparticles formation and its characterization. *Adv. Mater. Lett.* **2011**, *2*, 313–317. [CrossRef]
55. Bhuyan, T.; Mishra, K.; Khanuja, M.; Prasad, R.; Varma, A. Biosynthesis of zinc oxide nanoparticles from *Azadirachta indica* for antibacterial and photocatalytic applications. *Mater. Sci. Semicond* **2015**, *32*, 55–61. [CrossRef]
56. Reddy, K.M.; Feris, K.; Bell, J.; Wingett, D.G.; Hanley, C.; Punnoose, A. Selective toxicity of zinc oxide nanoparticles to prokaryotic and eukaryotic systems. *Appl. Phys. Lett.* **2007**, *90*, 213902. [CrossRef]
57. Zarrindokht, E.K.; Pegah, C. Antibacterial activity of ZnO nanoparticle on gram-positive and gram-negative bacteria. *Afr. J. Microbiol. Res.* **2011**, *5*, 1368–1373. [CrossRef]
58. Schwartz, V.B.; Thétiot, F.; Ritz, S.; Pütz, S.; Choritz, L.; Lappas, A.; Förch, P.; Landfester, K.; Jonas, U. Antibacterial surface coatings from zinc oxide nanoparticles embedded in poly (n-isopropylacrylamide) hydrogel surface layers. *Adv. Funct. Mater.* **2012**, *22*, 2376–2386. [CrossRef]
59. Wahab, R.; Siddiqui, M.A.; Saquib, Q.; Dwivedi, S.; Ahmad, J.; Musarrat, J.; Al-Khedhairi, A.A.; Shin, H.S. ZnO nanoparticles induced oxidative stress and apoptosis in HepG2 and MCF-7 cancer cells and their antibacterial activity. *Colloids Surf. B Biointerfaces* **2014**, *117*, 267–276. [CrossRef] [PubMed]
60. Xie, Y.; He, Y.; Irwin, P.L.; Jin, T.; Shi, X. Antibacterial activity and mechanism of action of zinc oxide nanoparticles against *Campylobacter jejuni*. *Appl. Environ. Microbiol.* **2011**, *77*, 2325–2331. [CrossRef] [PubMed]
61. Shi, L.E.; Li, Z.H.; Zheng, W.; Zhao, Y.F.; Jin, Y.F.; Tang, Z.X. Synthesis, antibacterial activity, antibacterial mechanism and food applications of ZnO nanoparticles: A review. *Food Addit. Contam.* **2014**, *31*(Part A), 173–186. [CrossRef]

62. Wills, R.; Golding, J. *Postharvest: An Introduction to the Physiology and Handling of Fruit and Vegetables*, 6th ed.; CABI: Wallingford, UK, 2016; 293p. [[CrossRef](#)]
63. Ali, A.; Maqbool, M.; Ramachandran, S.; Alderson, P.G. Gum arabic as a novel edible coating for enhancing shelf-life and improving postharvest quality of tomato (*Solanum lycopersicum* L.) fruit. *Postharvest Biol. Technol.* **2010**, *58*, 42–47. [[CrossRef](#)]
64. Kanmani, P.; Rhim, J.W. Properties and characterization of bionanocomposite films prepared with various biopolymers and ZnO nanoparticles. *Carbohydr. Polym.* **2014**, *106*, 190–199. [[CrossRef](#)] [[PubMed](#)]
65. Abdel-Aziz, M.S.; Salama, H.E. Development of alginate-based edible coatings of optimized UV-barrier properties by response surface methodology for food packaging applications. *Int. J. Biol. Macromol.* **2022**, *212*, 294–302. [[CrossRef](#)] [[PubMed](#)]
66. Saekow, M.; Naradisorn, M.; Tongdeesontorn, W.; Hamauzu, Y. Effect of carboxymethyl cellulose coating containing ZnO nanoparticles for prolonging shelf life of persimmon and tomato fruit. *J. Food Sci. Agric. Technol.* **2019**, *5*, 41–48.
67. Meng, X.; Zhang, M.; Adhikari, B. The effects of ultrasound treatment and nano-zinc oxide coating on the physiological activities of fresh-cut kiwifruit. *Food Bioproc. Technol.* **2014**, *7*, 126–132. [[CrossRef](#)]
68. Silva, G.M.C.; Silva, W.B.; Medeiros, D.B.; Salvador, A.R.; Cordeiro, M.H.M.; da Silva, N.M.; Santana, D.B.; Mizobutsi, G.P. The chitosan affects severely the carbon metabolism in mango (*Mangifera indica* L. cv. Palmer) fruit during storage. *Food Chem.* **2017**, *237*, 372–378. [[CrossRef](#)] [[PubMed](#)]
69. Diaz-Mula, H.M.; Serrano, M.; Valero, D. Alginate coatings preserve fruit quality and bioactive compounds during storage of sweet cherry fruit. *Food Bioproc. Technol.* **2012**, *5*, 2990–2997. [[CrossRef](#)]
70. Kittur, F.S.; Saroja, N.; Habibunnisa; Tharanathan, R. Polysaccharide-based composite coating formulations for shelf-life extension of fresh banana and mango. *Eur. Food Res. Technol.* **2001**, *213*, 306–311. [[CrossRef](#)]
71. Yaman, Ö.; Bayoandurl, L. Effects of an edible coating and cold storage on shelf-life and quality of cherries. *LWT-Food Sci. Technol.* **2002**, *35*, 146–150. [[CrossRef](#)]
72. Nawab, A.; Alam, F.; Hasnain, A. Mango kernel starch as a novel edible coating for enhancing shelf-life of tomato (*Solanum lycopersicum*) fruit. *Int. J. Biol. Macromol.* **2017**, *103*, 581–586. [[CrossRef](#)] [[PubMed](#)]
73. Wu, J.; Sun, Q.; Huang, H.; Duan, Y.; Xiao, G.; Le, T. Enhanced physico-mechanical, barrier and antifungal properties of soy protein isolate film by incorporating both plant-sourced cinnamaldehyde and facile synthesized zinc oxide nanosheets. *Colloids Surf. B Biointerfaces* **2019**, *180*, 31–38. [[CrossRef](#)]
74. Emamifar, A.; Bavaisi, S. Nanocomposite coating based on sodium alginate and nano- ZnO for extending the storage life of fresh strawberries (*Fragaria × ananassa* Duch.). *J Food Meas Charact.* **2020**, *14*, 1012–1024. [[CrossRef](#)]
75. Elsheshetawy, H.E.; Mossad, A.; Elhelew, W.K.; Farina, V. Comparative study on the quality characteristics of some Egyptian mango cultivars used for food processing. *Ann. Agric. Sci.* **2016**, *61*, 49–56. [[CrossRef](#)]
76. Mditshwa, L.S.; Magwaza, S.Z.; Tesfay, N. Mbili Postharvest quality and composition of organically and conventionally produced fruits: A review. *Sci. Hortic.* **2017**, *216*, 148–159. [[CrossRef](#)]
77. Thakur, R.; Pristijono, P.; Bowyer, M.; Singh, S.P.; Scarlett, C.J.; Stathopoulos, C.E.; Vuong, Q.V. A starch edible surface coating delays banana fruit ripening. *LWT-Food Sci. Technol.* **2019**, *100*, 341–347. [[CrossRef](#)]
78. Gol, N.B.; Chaudhari, M.L.; Rao, T.V.R. Effect of edible coatings on quality and shelf life of carambola (*Averrhoa carambola* L.) fruit during storage. *J. Food Sci. Technol.* **2015**, *52*, 78–91. [[CrossRef](#)]
79. Batista-Silva, W.; Nascimento, V.L.; Medeiros, D.B.; Nunes-Nesi, A.; Ribeiro, D.M.; Zsögön, A.; Araújo, W.L. Modifications in organic acid profiles during fruit development and ripening: Correlation or causation? *Front. Plant Sci.* **2018**, *9*, 1689. [[CrossRef](#)]
80. Xu, D.; Qin, H.; Ren, D. Prolonged preservation of tangerine fruits using chitosan/montmorillonite composite coating. *Postharvest Biol. Technol.* **2018**, *143*, 50–57. [[CrossRef](#)]
81. Prasanna, V.; Prabha, T.N.; Tharanathan, R.N. Fruit ripening phenomena—an overview. *Crit. Rev. Food Sci. Nutr.* **2007**, *47*, 231–258. [[CrossRef](#)]
82. Cordenunsi, B.R.; Lajolo, F.M. Starch breakdown during banana ripening: Sucrose synthase and sucrose phosphate synthase. *J. Agric. Food Chem.* **1995**, *43*, 347–351. [[CrossRef](#)]
83. Osorio, S.; Scossa, F.; Fernie, A. Molecular regulation of fruit ripening. *Front. Plant Sci.* **2013**, *4*, 198. [[CrossRef](#)]
84. Khaliq, G.; Mohamed, M.T.M.; Ali, A.; Ding, P.; Ghazali, H.M. Effect of gum arabic coating combined with calcium chloride on physico-chemical and qualitative properties of mango (*Mangifera indica* L.) fruit during low temperature storage. *Sci. Hortic.* **2015**, *190*, 187–194. [[CrossRef](#)]
85. Swallah, M.S.; Sun, H.; Affoh, R.; Fu, H.; Yu, H. Antioxidant potential overviews of secondary metabolites (polyphenols) in fruits. *Int. J. Food Sci.* **2020**, *2020*, 9081686. [[CrossRef](#)]
86. Tanada-Palmu, P.S.; Grosso, C.R. Effect of edible wheat gluten-based films and coatings on refrigerated strawberry (*Fragaria ananassa*) quality. *Postharvest Biol. Technol.* **2005**, *36*, 199–208. [[CrossRef](#)]

Disclaimer/Publisher’s Note: The statements, opinions and data contained in all publications are solely those of the individual author(s) and contributor(s) and not of MDPI and/or the editor(s). MDPI and/or the editor(s) disclaim responsibility for any injury to people or property resulting from any ideas, methods, instructions or products referred to in the content.